2002

Cell Surface-localized Nucleolin Is a Eukaryotic Receptor for the Adhesin Intimin-γ of Enterohemorrhagic *Escherichia coli* O157:H7

James F. Sinclair
Uniformed Services University of the Health Sciences

Alison D. O'Brien
Uniformed Services University of the Health Sciences

THE JOURNAL OF BIOLOGICAL CHEMISTRY Vol. 277, No. 4, Issue of January 25, pp. 2876–2885, 2002
Printed in U.S.A.

Cell Surface-localized Nucleolin Is a Eukaryotic Receptor for the Adhesin Intimin-γ of Enterohemorrhagic *Escherichia coli* O157:H7*

Received for publication, October 24, 2001
Published, JBC Papers in Press, November 9, 2001, DOI 10.1074/jbc.M110230200

James F. Sinclair and Alison D. O'Brien‡

From the Department of Microbiology and Immunology, Uniformed Services University of the Health Sciences, Bethesda, Maryland 20814-4799

Intimin-γ is an outer membrane protein of enterohemorrhagic *Escherichia coli* (EHEC) O157:H7 that is required for the organism to adhere tightly to HEp-2 cells and to colonize experimental animals. Another EHEC O157:H7 protein, the Transferred intimin receptor (Tir), is considered the primary receptor for intimin-γ. Nevertheless, Tir-independent binding of intimin-γ to HEp-2 cells has been reported. This observation suggests the existence of a eukaryotic receptor(s) for intimin-γ. In this study, we sought to identify that receptor(s). First, we determined by equilibrium binding titration that the association of purified intimin-γ with HEp-2 cells was specific and consistent with a single host cell receptor. Second, we isolated a protein from lysates of HEp-2 cells that bound intimin-γ and subsequently identified this molecule as nucleolin, a protein involved in cell growth regulation that can be cell surface-expressed. Third, we established that purified intimin-γ and nucleolin were co-localized on the surface of HEp-2 cells and that the site of EHEC O157:H7 attachment was associated with regions of nucleolin expression. Finally, we demonstrated that mouse anti-nucleolin sera significantly decreased the adherence of EHEC O157:H7 to HEp-2 cells. From this, we conclude that nucleolin is the HEp-2 cell receptor for intimin-γ expressed by EHEC O157:H7.

Escherichia coli that make one or more types of Shiga toxin (collectively called Shiga toxin-producing *E. coli* (STECs))[1] are estimated to cause 110,000 diarrheal illnesses a year in the United States (1). *E. coli* O157:H7 is responsible for about 74,000 of these cases. *E. coli* O157:H7 belongs to a subset of STEC designated enterohemorrhagic *E. coli* (or EHEC) that not only makes Shiga toxins but also produces a protein called intimin (2) that facilitates the organisms attachment to the lumen of the bowel and evokes an attach and efface lesion at the site of the bacterial-enterocyte interface (3). The genes for production of the A/E lesion, which include intimin and Tir (4), are located on an ~43-kb pathogenicity island in the O157:H7 chromosome called the locus of enterocyte effacement (LEE) (5). In addition to intimin and Tir, the LEE contains genes for a type III secretion system (6) as well as for a number of *E. coli*-secreted proteins that, along with Tir, are injected into the host cell (reviewed in Ref. 7). Acting in concert, these proteins expressed from the LEE induce the host cell to produce an actin-rich pedestal that appears to cup the bacterium and anchor it into place (reviewed in Ref. 8).

EHEC O157:H7 intimin belongs to a family of adhesin molecules that are produced by bacteria capable of evoking A/E lesions, *i.e.* enteropathogenic *E. coli* (EPEC), *Hafnei alvei, Citrobacter rodentium,* as well as EPEC-like bacteria of rabbits and dogs (3, 9, 10). Members of the intimin family of adhesins are also related to the invasins of *Yersinia enterocolitica* and *Yersinia pseudotuberculosis* (11). Not all regions of the intimins and invasin share equivalent amino acid sequence homologies. Indeed, the transmembrane domains of these proteins are relatively conserved, but the sequences of the carboxyl-terminal regions that contain the putative host cell binding domain are divergent (12, 13). For the *Yersinia* invasins, these carboxyl-terminal regions bind to the eukaryotic β_1 integrin receptor (14), whereas for the EPEC and EHEC O157:H7 intimins the carboxyl-terminal domain is required for direct binding to the LEE-encoded intimin receptor Tir (15). Currently, intimins have been classified into at least five different types (α, β, γ, δ, and ε) based on homologies in the carboxyl termini of the proteins (16, 17). The intimin of EHEC O157:H7 is of the gamma type and will hereafter be designated intimin-γ.

Several lines of evidence indicate that intimin-γ is the primary adhesin of EHEC O157:H7. First, intimin-γ is required for adherence of EHEC O157:H7 to tissue culture cells and human pediatric explants (18–20). Second, the protein is necessary for EHEC O157:H7-evoked A/E lesion formation and intestinal colonization of gnotobiotic pigs and colostrum-deprived calves (21–23). Third, disruption of the intimin-γ *eae* gene abolishes adherence of EHEC (18). Fourth, antiserum raised against intimin-γ blocks binding of EHEC O157:H7 to cultured epithelial cells (22–24). The probable role of intimin-γ as an adherence factor for EHEC O157:H7 has prompted an intense search for its putative host cell receptor. Based on both the homology between invasin and the intimins and the capacity of invasin to mediate *Y. enterocolitica* and *Y. pseudotuberculosis* invasion of the host cells by binding to β_1 chain integrins (14), the integrin-binding properties of intimins have been investigated. Although intimins can bind to β_1 chain integrins in enzyme-linked immunosorbent assays or on the surface of lymphocytes (27), the current consensus in the literature is that intimin association with β_1 chain integrins is not essential for adherence (28). Rather, Finlay and co-workers (4, 29) convincingly demonstrated that EPEC intimin-α as well as EHEC O157:H7 intimin-γ bind to the cognate bacterial Tir

* This work was supported by Grants AI20148-16 from the National Institutes of Health and by 97-35201-4578 from the United States Department of Agriculture. The costs of publication of this article were defrayed in part by the payment of page charges. This article must therefore be hereby marked "*advertisement*" in accordance with 18 U.S.C. Section 1734 solely to indicate this fact.

‡ To whom correspondence should be addressed: Dept. of Microbiology and Immunology, Uniformed Services University of the Health Sciences, 4301 Jones Bridge Rd., Bethesda, MD 20814-4799. Tel.: 301-295-3419; Fax: 301-295-3773; E-mail: aobrien@usuhs.mil.

[1] The abbreviations used are: STEC, Shiga toxin-producing *E. coli*; EHEC, enterohemorrhagic *E. coli*; EPEC, enteropathogenic *E. coli*; A/E, attach and efface; Tir, translocated intimin receptor; LEE, locus of enterocyte effacement; GFP, green fluorescent protein; EMEM, Eagle's minimal essential medium; HRP, horseradish peroxidase; FITC, fluorescein isothiocyanate; PBS, phosphate-buffered saline.

protein that is injected into the host cell by the bacteria. However, the pattern of phosphorylation of EHEC O157:H7 Tir after injection into the host cell is different from that of EPEC Tir, an observation that may suggest differences in the function of these proteins within the eukaryotic cell (29). Disruption of the *tir* gene in both EPEC and EHEC abolishes adherence, and this finding supports the critical role of the interaction between Tir and intimin during infection (4, 29).

That intimin binds to Tir on the host cell surface is incontrovertible. Nevertheless, there is also indirect evidence for a eukaryotic intimin receptor. The findings in favor of such a cellular receptor are as follows. First, enteropathogenic and enterohemorrhagic *E. coli* preferentially colonize different portions of the gastrointestinal tract, *i.e.* these microbes infect the small intestine and large intestine, respectively (3). This specific tissue tropism appears to be influenced by intimin, as work by Tzipori *et al*. (21) has shown that in gnotobiotic pigs the location of EPEC colonization can be altered based on the type of intimin (EPEC intimin-α or EHEC intimin-γ) the bacteria express. Furthermore, experiments with human intestinal tissue demonstrate that bacteria that express intimin-γ adhere selectively to the follicle-associated epithelium above the Peyer's patches, whereas the same bacteria that express intimin-α adhere to both the small intestinal mucosa and the follicle-associated epithelium of Peyer's patches (30). Second, as inferred earlier, the genetic sequences that encode the host cell binding domains of the different intimin types are far more divergent than the surrounding, more conserved sequences (31). The sequence divergence in the host cell binding regions of the intimins most likely represents changes advantageous for colonization of a particular niche by the different LEE-containing bacteria (12, 13). A final line of evidence that suggests that intimin may have a host cell surface receptor other than Tir comes from mutational analysis of the host cell binding domain of intimin-α. Mutations in this region of the adhesin disrupt the capacity of the bacteria to adhere to the host cell but do not interfere with the *in vitro* interaction between intimin and Tir (32, 33). If Tir functions as the sole intimin receptor, such mutations should not affect bacterial adherence. One caveat to this interpretation is that these mutations may not disrupt binding *in vitro* but may destabilize the interaction between intimin and Tir *in vivo* sufficiently to prevent adherence (34).

If intimin does bind to a eukaryotic receptor in a manner analogous to that of the invasin-integrin interaction, then purified intimin should bind to the surface of host cells. In fact, several groups have investigated the binding of purified intimin to tissue culture cells with varying results. Frankel and colleagues (12, 35) reported that fusion proteins that contained the carboxyl-terminal domain of intimin bind in a punctate manner across the HEp-2 cell surface, whereas De Vinney *et al*. (29) and Liu *et al*. (36) have found that purified intimin does not bind to HeLa cells unless Tir is first inserted into the host cell membrane by preinfection with an intimin-deletion strain. In accordance with the methodology described by Frankel *et al*. (12), our experience has been that both holointimin-γ and its carboxyl-terminal domain alone can bind to HEp-2 tissue culture cells in the absence of Tir.[2] For the research presented in this paper, our goals were to quantify the binding of purified intimin-γ to HEp-2 cells, identify the intimin-γ receptor on the cells, and determine whether this interaction is of biological significance with respect to the adherence of EHEC O157:H7 to these epithelial cells.

[2] L. J. Gansheroff and A. D. O'Brien, unpublished data.

EXPERIMENTAL PROCEDURES

Bacterial Strains and Plasmids—EHEC O157:H7 strain 86-24 was isolated in 1986 from a patient in Seattle, WA and was kindly provided by Dr. Phil Tarr (Children's Hospital and Medical Center, Seattle, WA). DNA isolated from this strain served as a template for amplification of both the *eae* (intimin-γ) and *tir* genes. The histidine-tagged expression plasmids pEB313 (encodes all but the first 34 amino acids (potential signal sequence) of the *eae* gene) and pMW103 (encodes the carboxyl-terminal third of intimin) as well as the *E. coli* strain L172 that was used for overexpression of intimin-γ proteins have been described previously (24, 37). The entire *tir* gene with some flanking sequence was amplified from EHEC O157:H7 strain 86-24 by PCR with primers that incorporated *Xba*I restriction sites into the wild-type sequence (31) (GTCATCTAGAGCCGTTTATCGACTACGTGC upstream and CAGAAGCTCTAGAGTTGCCATCC downstream). Restriction enzyme digest patterns of the PCR product were consistent with that of the published sequence for *tir* (31). The fragment was then ligated into pBluescript II KS (Stratagene) to permit overexpression of the Tir protein. This construct was designated pTir and was subsequently transformed into the *E. coli* strain BL21 (Novagen) that contains a chromosomally encoded T7 polymerase gene under control of the *lac* repressor. Plasmid p166 was generously provided by Drs. William Day and Anthony Maurelli (Uniformed Services University of the Health Sciences, Bethesda, MD). This pBAD-based plasmid (38) contains the gene for the green fluorescent protein (39) inserted behind an arabinose-inducible promoter. Plasmid p166 was transformed into EHEC strain 86-24 by electroporation. GFP expression was induced with 1% arabinose and was used as a means of visualizing bacterial adherence to HEp-2 cells (see "Bacterial Adherence Assay" below for details).

Culture Cell—HEp-2 (ATCC CCL23) human laryngeal epithelial cells were maintained by serial passage in EMEM (BioWhittaker), supplemented with 10% fetal calf serum, 20 mM L-glutamine, 100 μg/ml gentamicin, 10 units/ml penicillin G, and 10 μg/ml streptomycin (called complete EMEM). Cells were grown at 37 °C in a humidified atmosphere of 5% CO_2. For subconfluent HEp-2 cell monolayers, 8-well chamber slides (Lab-Tek) were seeded with 6×10^4 cells/well in complete EMEM and incubated for no more than 24 h (~80% confluent) before use. Confluent HEp-2 cell monolayers were prepared according to a method previously described for Vero cells (40). HEp-2 cells were seeded into 8-well chamber slides at a density of 3×10^4 cells/well and incubated for 72 h. The medium in each well was then removed and replaced with complete EMEM that contained 1% fetal calf serum. Cells were maintained under these conditions for up to 48 h prior to use.

Protein Purification—Luria broth cultures (250 ml) of *E. coli* strain L172 transformed with pEB313, pMW103, or *E. coli* strain BL21 transformed with pTir were grown at 37 °C to an optical density ($A_{600\ nm}$) of 0.8, and protein was expression induced by the addition of 1 mM isopropyl-β-thiogalactopyranoside. Four h after induction, the bacteria were harvested by centrifugation and lysed by the addition of 5 M guanidine hydrochloride, pH 8. Insoluble protein was removed from the lysate by centrifugation. Proteins were then purified from the clarified lysates as follows. Each histidine-tagged intimin-γ protein was purified by passage over a nickel affinity resin (Ni-NTA, Qiagen). Columns were washed with 10 column volumes of 8 M urea, pH 8, followed by 10 column volumes of 8 M urea, pH 6.5. Tagged proteins were eluted by the addition of 2 column volumes of 8 M urea, pH 4.5. The eluted proteins were dialyzed thoroughly against 100 mM sodium phosphate monobasic buffer at pH 4.5, which allowed intimin-γ to remain soluble at high concentration. Proteins were stored frozen at −20 °C in dialysis buffer until needed. The concentrations of the histidine-tagged intimin-γ proteins were determined by absorbance at 280 nm using an extinction coefficient of 119710 $M^{-1}\ cm^{-1}$ calculated from the amino acid composition of the intimin-γ sequence. Please note that for purposes of brevity, these nickel affinity-purified, histidine-tagged intimin-γ proteins are referred to in this article as intimin-γ or intimin-γ carboxyl-terminal third. We have no reason to suspect that addition of the histidine tag at the amino terminus of the proteins alters in any way the adhesion mediated by the carboxyl-terminal extracellular domain of intimin.

The Tir protein was extracted from isopropyl-β-thiogalactopyranoside-induced cultures with 5 M urea and concentrated from clarified lysates by 60% ammonium sulfate precipitation, and the precipitate was dialyzed against 100 mM sodium phosphate buffer, pH 7. The dialysate was then subjected to anion-exchange column chromatography with DEAE-Sephadex A-50 (Amersham Biosciences, Inc.). Protein was eluted from the column with 0.45 M NaCl and was ~80% pure as assessed by SDS-PAGE.

Nucleolin was purified from HEp-2 cells as follows. Cells were lysed

in 10 mM phosphate buffer, pH 6.5, that contained 250 mM NaCl, 0.5% Triton X-100, and 150 μg/ml phenylmethylsulfonyl fluoride (Roche Molecular Biochemicals). Soluble nucleolin was extracted from solution with DEAE Sephadex A-50 (Amersham Biosciences, Inc.) and eluted from the resin with lysis buffer that contained 500 mM NaCl. Eluted proteins were precipitated with 30% ammonium chloride and dialyzed against 50 mM phosphate buffer, pH 6.5, that contained 250 mM NaCl. The dialysate was then subjected to DEAE-Sepharose CL-6B (Amersham Biosciences, Inc.) anion-exchange column chromatography. The column was washed with phosphate buffer containing 300 mM NaCl, and protein was eluted from the column with a linear salt gradient from 300 to 500 mM NaCl. Fractions that contained the highest concentration of nucleolin were pooled. This material appeared homogeneous on Coomassie-stained SDS-PAGE and ran as one spot on a two-dimensional gel.

Antibodies and Production of Antisera—An IgG monoclonal antibody against intimin-γ was prepared in collaboration with Virion Systems Inc. (Rockville, MD)[3] Polyclonal antiserum against intimin-γ was produced in conjunction with Duncroft, Inc. (Lovettsville, VA) by immunization of a sheep with purified intimin-γ mixed with Freund's adjuvant.[4] Anti-nucleolin monoclonal antibody C23 (MS-3) was purchased from Santa Cruz Biotechnology, Inc. Polyclonal antibodies against HEp-2 cell nucleolin were raised in 6–8-week-old BALB/c female mice by intraperitoneal injection of protein eluted from an SDS-polyacrylamide gel slice and mixed with adjuvant. Serum samples from mice were tested by Western blot analysis for reactivity to HEp-2 cell nucleolin, and immunoreactive serum samples were pooled. Normal mouse serum was obtained from nonimmunized mice of the same lot. In conjunction with Cocalico Biologicals, Inc. (Reamstown, PA), polyclonal antiserum against Tir was produced in a rabbit by subcutaneous injection of electroeluted Tir mixed with adjuvant. Secondary antibodies were obtained from the following suppliers: HRP-conjugated goat anti-mouse IgG from Bio-Rad Laboratories; FITC-conjugated goat anti-mouse IgG and Texas Red-conjugated donkey anti-sheep IgG from Jackson ImmunoResearch Laboratories.

Immunoblot Analysis and Protein Overlay Assays—Proteins used in this study were separated by molecular weight using SDS-PAGE with a Mini-PROTEAN II Electrophoresis Cell (Bio-Rad) following standard protocols. For two-dimensional electrophoresis, detergent-solubilized HEp-2 proteins were separated in the first dimension by isoelectric focusing using the Mini-PROTEAN Tube Cell (Bio-Rad) and then in the second dimension by SDS-PAGE. Protein gels were blotted onto Optitran nitrocellulose membranes (Schleicher & Schuell) with a Trans-Blot SD Semi-Dry Electrophoretic Transfer Cell (Bio-Rad). Membranes were blocked with PBS, pH 7.4, that contained 5% powdered milk and 0.2% Tween 20. For Western analyses, both primary and secondary antibodies were diluted in 5% powdered milk, 0.2% Tween 20 in PBS. The anti-nucleolin monoclonal antibody was used at a 1:5,000 dilution and the anti-intimin monoclonal antibody at a 1:7,000 dilution. The HRP-conjugated goat anti-mouse IgG secondary antibody was diluted 1:20,000. Immunoreactive proteins were detected with enhanced chemiluminescence (ECL Plus, Amersham Biosciences, Inc.). For intimin-γ protein overlay assays, purified intimin-γ was diluted to a concentration of 3 μg/ml in PBS, pH 6.5 that contained 2% powdered milk and 0.2% Tween 20. This solution was incubated with blots of SDS-PAGE separated HEp-2 proteins that were not heated or reduced before electrophoresis. Intimin-γ that had bound to specific HEp-2 cell proteins was detected with anti-intimin monoclonal antibodies as described above. For nucleolin protein overlay assays, HEp-2 cells were extracted with 50 mM phosphate buffer pH 8 that contained 0.1% Triton X-100, and the soluble proteins were diluted into PBS, pH 6.5, that contained 2% powdered milk and 0.2% Tween 20. This solution was incubated with immunoblots of intimin-γ (full-length and carboxyl-terminal third) that had been separated by SDS-PAGE without heating or reduction of the samples. Nucleolin from the HEp-2 extract that had bound to intimin-γ or the carboxyl-terminal third of intimin-γ was detected with anti-nucleolin monoclonal antibodies per the above protocol.

Intimin-γ Affinity Chromatography—Intimin-γ was covalently linked by means of 1-ethyl-3-(3-dimethylaminopropyl)-carbodiimiide hydrochloride (Sigma) to carboxylate-modified polystyrene particles (Seradyn, Inc.). Bovine serum albumin was covalently linked to the same type of particles as a control to assess the level of nonspecific binding of HEp-2 cell extracts to that matrix. HEp-2 cells were lysed in a 10 mM phosphate buffer, pH 8, that contained 136 mM NaCl, 1 mM MgCl, 0.5 mM CaCl, 0.5% Triton X-100, and 150 μg/ml phenylmethylsulfonyl fluoride. The pH of the cell extract was then reduced to 6 by a dropwise addition of HCl. Insoluble protein was removed by centrifugation, and the clarified supernatant was mixed gently with the intimin-γ–linked polystyrene particles for 1 h at 25 °C. The particles were removed from solution and washed extensively with buffer. HEp-2 cell proteins that had bound to intimin-γ were eluted by rinsing particles with a 50 mM phosphate buffer, pH 7, that contained 250 mM NaCl. Eluted proteins were separated by SDS-PAGE and stained with Coomassie Brilliant Blue.

Protein Sequencing—A HEp-2 cell protein with an apparent molecular mass of 110 kDa was selected for amino acid sequencing because it displayed the most intense immunoreactive band in intimin-γ protein overlay assays. Following intimin-γ affinity purification, this protein was excised from an SDS-polyacrylamide gel and sent to the Protein Chemistry Laboratory, Department of Biochemistry, Texas A&M University. In that laboratory, the protein in the gel slice was reduced, alkylated, and digested with Endo-LysC. Peptides were extracted and purified by reverse-phase, narrow bore, high-pressure liquid chromatography. The purified peptides were then subjected to automated Edman protein sequencing on a Hewlett Packard G1000A Automated Protein Sequencer. Peptide sequences obtained by these methods were used as input for a BLAST search (41) of the available data bases.

Intimin-γ Binding to HEp-2 Cells—Purified intimin-γ was labeled with biotinamidocaproate *N*-hydroxysuccinimide ester (Sigma) in 0.1 M sodium borate buffer, pH 9, at a ratio of 1 μg of ester/25 μg of protein. Samples were incubated at room temperature for 2 h, and then the reaction was stopped by the addition of 5 mM ammonium chloride. Excess label was removed by extensive dialysis of the mixture against 50 mM phosphate buffer, pH 5. Labeled intimin-γ was diluted into RPMI 1640 medium that contained 20 mM sodium phosphate monobasic and 0.5% bovine serum albumin (Sigma). For the titration of intimin-γ binding to HEp-2 cells, 96-well tissue culture plates (Costar) were seeded with 2×10^4 cells/well in complete EMEM and used 24 or 48 h later. Intimin-γ over a range of concentrations (0.05–50 μg/ml) was incubated with these cells for 1 h. In a separate experiment, labeled intimin-γ at the same range of concentrations was incubated with HEp-2 cells in the presence of a large excess (500 μg/ml) of unlabeled intimin-γ under the same conditions. Unbound protein was then removed from all wells by aspiration and the cells washed gently with PBS. Bound protein and HEp-2 cells were removed from the wells by the addition of SDS sample buffer (25 mM Tris, pH 6.8, 1% SDS, 5% glycerol). Total protein from the wells was separated by SDS-PAGE and blotted onto nitrocellulose. Labeled intimin-γ that had bound to the HEp-2 cell surface was visualized by incubation of the blots with a streptavidin-HRP conjugate (Amersham Biosciences, Inc.) diluted 1:10,000 in PBS with 5% powdered milk and 0.2% Tween 20, followed by chemiluminescent detection and autoradiography as described above. To generate a standard curve against which to estimate the concentration of intimin-γ bound to HEp-2 cells, various concentrations of labeled intimin-γ were subjected to SDS-PAGE and then immunoblotted. Autoradiographs of the intimin Western blots were digitized and the protein concentration determined by densitometric analysis performed on a Macintosh computer using the public domain NIH Image program (developed at the National Institutes of Health).[5]

Bacterial Adherence Assay—Infection of HEp-2 cells with EHEC strain 86-24 was done essentially as described previously (37) with minor modifications. HEp-2 cell monolayers were infected with strain 86-24 taken from a Luria broth static overnight culture and diluted into EMEM that contained 1% mannose and 10 mM sodium phosphate. After 2.5–3 h of infection, cells were washed with PBS to remove nonadherent bacteria and fresh EMEM buffer was added. After an additional 3 h of incubation, the infected cells were washed thoroughly with PBS to remove all bacteria that were not intimately adherent. Cells were then fixed with 3% formalin for 20 min. For some experiments, the cells were then permeabilized with 0.1% Triton X-100 for 4 min. To induce GFP expression in bacteria that had been transformed with p166, 1% arabinose was substituted for 1% mannose in the adherence buffer. For antibody blocking experiments, anti-nucleolin and normal mouse sera were diluted 1:100 in adherence medium. Identical samples of anti-nucleolin and normal mouse sera were selectively depleted of anti-nucleolin antibodies by adsorption on strips of nitrocellulose that contained purified nucleolin protein. Antibodies specific for nucleolin were eluted from the nitrocellulose strips by the addition of 100 mM glycine

[3] M. R. Wachtel, L. J. Gansheroff, R. F. Schuman, and A. D. O'Brien, unpublished data.

[4] M. Mills, E. M. Twiddy, and A. D. O'Brien, unpublished data.

[5] Available on the Internet at rsb.info.nih.gov/nih-image/.

buffer, pH 2, followed by neutralization of the eluted material with 100 mM Tris buffer, pH 8. All samples (polyclonal sera, depleted sera, and eluted antibodies) were heated to 56 °C for 30 min to inactivate complement. These samples were then added to cells 1 h prior to infection with strain 86-24(p166). Four h after infection, nonadherent bacteria were washed from the cells. The number of adherent GFP-expressing bacteria were counted from an image obtained under fluorescence.

Indirect Immunofluorescence Microscopy—Nucleolin expressed on the surface of HEp-2 cells was detected as follows. Mouse anti-nucleolin polyclonal sera (pooled from 4 mice) were diluted 1:100 into culture medium and added to cells for at least 1 h. Cells were then formalin fixed and, if necessary, permeabilized. Anti-nucleolin antibodies were detected by incubation for 1 h with a FITC-conjugated goat anti-mouse IgG antibody diluted 1:40 in PBS that contained 3% bovine serum albumin. To demonstrate intimin-γ binding to cells, 5 μg/ml purified intimin-γ was incubated with HEp-2 cells as described above. After cells were formalin-fixed, sheep anti-intimin-γ diluted 1:50 in PBS that contained 3% bovine serum albumin was added to the cells for 1 h. Intimin-γ-anti-intimin complexes were detected by incubation of the cells for 1 h with Texas Red-conjugated donkey anti-sheep IgG-specific antibodies that had been diluted 1:40 in PBS with 3% bovine serum albumin. Tir localized beneath adherent bacteria or intimin-γ on the surface of adherent bacteria were detected as follows. HEp-2 cells were infected with EHEC strain 86-24 as described above. Following formalin fixation and Triton X-100 permeabilization, infected cells were incubated for 1 h with either sheep anti-intimin-γ or rabbit anti-Tir sera diluted 1:50 or 1:400, respectively, in PBS with 3% bovine serum albumin. Bound antibodies were then detected with the appropriate Texas Red-conjugated secondary antibody diluted in the same buffer. Samples in this research were examined with an Olympus BX60 system microscope with a BX-FLA reflected light fluorescence attachment. All images were obtained with a SPOT RT CCD digital camera (Diagnostic Instrument, Inc.).

RESULTS

Quantitation of Intimin-γ Binding to the HEp-2 Cell Surface—To begin to define the interaction between intimin-γ and any potential eukaryotic receptor, we analyzed the association between biotin-labeled intimin-γ and HEp-2 cells over a range of protein concentrations. Examination of the kinetics of association for intimin-γ with HEp-2 cells (data not shown) demonstrated that equilibrium between the bound and free protein was established after ~40 min. Therefore, biotinylated intimin-γ was incubated with the cells for 1 h in all subsequent binding studies to provide sufficient time to establish equilibrium between the bound and free protein. The amount of biotinylated intimin-γ that bound to cells was determined by detection with a streptavidin-HRP conjugate. The binding of purified intimin-γ to subconfluent HEp-2 cells (24 h post-seeding) was saturable at the highest concentrations of purified protein tested (Fig. 1*A, closed circles*). In addition, these same concentrations of biotinylated intimin-γ were incubated with HEp-2 cells in the presence of excess (0.5 mg/ml) unlabeled intimin-γ (Fig. 1*A, open circles*) to provide an estimate of nonspecific binding. That the majority of labeled intimin-γ binding could be blocked by unlabeled protein suggests that the association between intimin-γ and the HEp-2 cell surface is specific. Scatchard analysis of this titration (Fig. 1*C, circles*) yielded a straight (non-curved) line, a finding that signified that intimin-γ bound to a single receptor. The slope of this line gave a dissociation constant of 84 nM (± 8 nM) for binding of purified intimin-γ to the surface of HEp-2 cells. HEp-2 cells used at 48 h post-seeding were fully confluent and bound significantly less purified intimin-γ than the subconfluent cells tested at 24 h (Fig. 1*B, closed squares*), whereas the amount of nonspecifically bound protein (Fig. 1*B, open squares*) was similar to that seen for the cells examined at 24 h post-seeding. The Scatchard plot of these data (Fig. 1*C, squares*) yielded a slope similar to that calculated for the binding of intimin-γ to subconfluent HEp-2 cells (93 nM (± 10 nM)). Based on the x-intercepts of the Scatchard plots for these two binding titrations, we estimated that the concentration of intimin-γ binding sites on the surface of confluent HEp-2 cells was ~50% lower than that present on the surface of subconfluent monolayers.

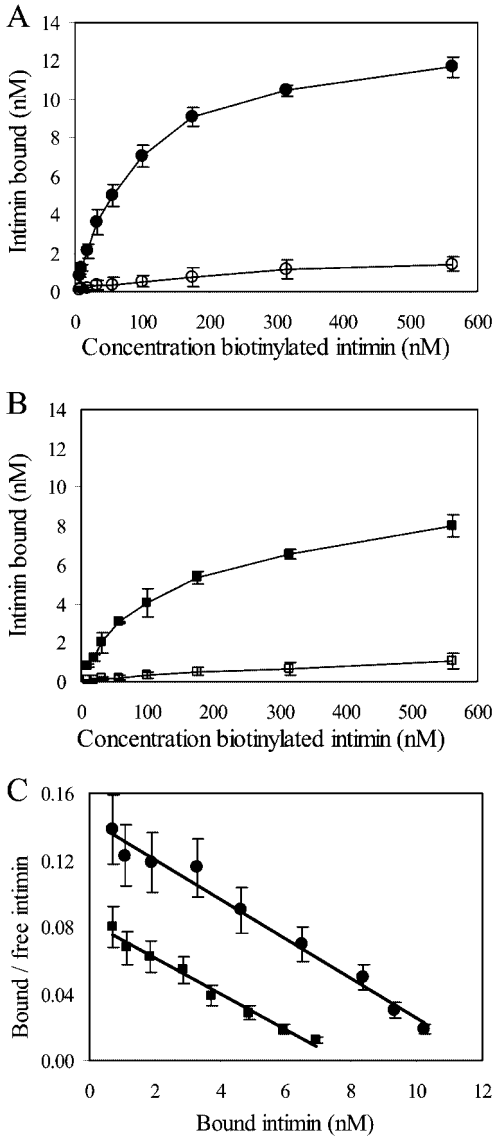

FIG. 1. **Titration of intimin-γ binding to the HEp-2 cell surface receptor.** A range of concentrations of biotinylated intimin-γ (*x* axis) was added to subconfluent (*A*) or confluent (*B*) monolayers of HEp-2 cells. These titrations were performed without (*closed symbols*) or with (*open symbols*) an excess (0.5 mg/ml) of unlabeled intimin-γ to provide an estimate of nonspecific binding. The concentration of biotinylated intimin-γ that bound to the cell surface (*y* axis) was determined as described under "Experimental Procedures." Each point is the mean of three independent measurements, and *error bars* depict one standard error of the mean. *C*, Scatchard plot of the binding data for biotinylated intimin-γ on subconfluent (*circles*) and confluent (*squares*) HEp-2 cell monolayers. The specifically bound protein concentration was calculated by subtracting the amount of nonspecifically bound protein (*open symbols*) from the total bound protein (*closed symbols*) in *panels A* and *B*. The slope of both lines gave an apparent dissociation constant of ~84–93 nM (±10 nM). The *error bars* represent 15% of the value of bound/free protein and indicate the maximum error of this calculation.

Identification of the HEp-2 Cell Receptor for Intimin-γ—Initially we made the assumption that the receptor for intimin-γ was most likely a protein or glycoprotein. Based on this prediction, we then used protein overlay assays as an initial approach to identify intimin-γ receptor candidates in HEp-2 cell extracts. For these studies, HEp-2 cell lysates were separated on SDS-polyacrylamide gels and the proteins blotted onto nitrocellulose. These blots were blocked and then incubated

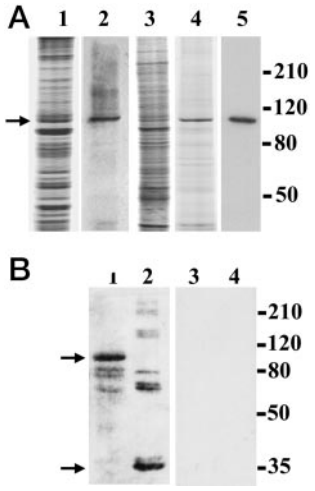

FIG. 2. **Purified intimin-γ or the carboxyl-terminal domain of intimin-γ bind preferentially to a HEp-2 cell protein identified as nucleolin.** *A,* extracts of HEp-2 cellular proteins were separated by SDS-PAGE and stained with Coomassie Blue (*lane 1*) or blotted onto nitrocellulose and used in protein overlay experiments with purified histidine-tagged intimin-γ (3 μg/ml). HEp-2 cell proteins that bound intimin-γ were detected with anti-intimin-γ monoclonal antibodies (*lane 2*). Coomassie Blue stained SDS-polyacrylamide gels of total Triton X-100-solubilized HEp-2 cell proteins before (*lane 3*) and after incubation and elution from an intimin-γ affinity matrix (*lane 4*). The protein that had the strongest affinity for intimin-γ was identified as nucleolin by internal amino acid sequencing. The same 110-kDa protein band recognized in *lanes 2* and *4* was detected by probing affinity-purified protein with a commercially available anti-nucleolin monoclonal antibody (*lane 5*). Molecular weight markers (in kDa) are indicated on the *right*; the *arrow* indicates the 110-kDa nucleolin protein. *B*, purified intimin-γ (*lanes 1* and *3*) or the carboxyl-terminal third of intimin-γ (*lanes 2* and *4*) were subjected to SDS-PAGE (without reducing agents), blotted onto nitrocellulose, and incubated with Triton X-100 soluble HEp-2 cell extracts that contained nucleolin (*lanes 1* and *2*) or with buffer (*lanes 3* and *4*). Bound nucleolin was detected with an anti-nucleolin monoclonal antibody. Molecular weight markers (in kDa) are indicated on the *right*; the *arrows* indicate intimin-γ (97 kDa) or the carboxyl-terminal third of intimin-γ (35 kDa).

with purified intimin-γ. After extensive washing, HEp-2 cell proteins to which intimin-γ had bound were detected with an anti-intimin-γ monoclonal antibody. Although numerous HEp-2 cell proteins were apparent in Coomassie Blue-stained gels (Fig. 2*A*, *lane 1*), only a few cellular proteins were found to bind intimin-γ (Fig. 2*A*, *lane 2*). In particular, one HEp-2 cell protein with an apparent molecular mass of 110 kDa produced an intense signal in overlay assays, a finding indicating that this protein species had bound significant amounts of purified intimin-γ. Several other proteins also bound intimin-γ, but the intensities of these signals were considerably less than that produced by the 110-kDa protein species (Fig. 2*A*, *lane 2*). These other signals may represent less avid or less specific binding of intimin-γ, and the identification of these proteins was not pursued further.

Next, we used affinity chromatography with intimin-γ as an adsorbent in an attempt to purify the HEp-2 cell receptor identified in protein overlay assays. Detergent-soluble HEp-2 cell proteins (Fig. 2*A*, *lane 3*) were incubated with intimin-γ linked to a solid support. The 110-kDa protein was eluted from the intimin-γ affinity matrix (Fig. 2*A*, *lane 4*) with an increase in salt concentration or an increase in pH. Binding of this 110-kDa protein was not observed on a control matrix that contained only covalently linked bovine serum albumin. The intimin-γ affinity matrix bound the greatest amount of the 110-kDa protein when incubated with HEp-2 cell extracts at a pH of 5.5 to 6, whereas no detectable binding of the 110-kDa protein to the matrix was evident at pH 8 or above. To identify the protein that bound to immobilized intimin-γ, the 110-kDa band was cut from a polyacrylamide gel and subjected to proteolytic cleavage, and two protein fragments were sequenced by Edman degradation. The sequences obtained for these two peptides were KGIAYIEFK and KEVFEDAAE. A BLAST search (41) of the relevant data bases with these peptide sequences revealed homology to the eukaryotic protein nucleolin. The peptide sequences we obtained were identical to human nucleolin (GenBank accession number AAA59954) between amino acids 410 and 437. Nucleolin has a predicted molecular mass of 77 kDa but has been reported to display an aberrant electrophoretic mobility of 110 kDa (42).

That we had identified nucleolin, a protein that functions in ribosome biogenesis and cell growth (reviewed in Refs. 42 and 43), as the putative HEp-2 cell receptor for intimin-γ was initially perplexing given that nucleolin is typically localized to the nucleolus of cells (44, 45). However, several reports have indicated that nucleolin can be expressed at the cell surface (46–49) and that surface-expressed nucleolin may serve as a cellular receptor for several viruses (50–52). Moreover, nucleolin is highly expressed and comprises up to 5% of the total nuclear protein in actively dividing cells, but its expression in the nucleus and on the cell surface of resting cells is largely down-regulated (45, 53, 54). The latter observation is in keeping with our finding that the binding of intimin-γ to HEp-2 cells is optimal in subconfluent cells and is decreased in confluent monolayers of cells (Fig. 1). For these reasons, we concluded that nucleolin was a credible candidate as a putative HEp-2 cell receptor for intimin-γ. Two findings from the isolation of nucleolin as the intimin-γ receptor lead us to believe that the association between these two proteins may involve electrostatic interactions. First, intimin-γ carries a large net positive charge (13), whereas nucleolin bears a large net negative charge (55). Second, the effects of salt and buffer pH on the binding and elution profile of nucleolin from the intimin-γ affinity matrix indicates that the disruption of electrostatic interactions interferes with the association between the two proteins.

To verify that the 110-kDa protein that bound to intimin-γ was nucleolin, a Western blot of the intimin-γ affinity-purified protein was probed with a commercially obtained monoclonal anti-nucleolin antibody (Fig. 2*A*, *lane 5*). From that immunoblot, we concluded that the protein eluted from the intimin-γ affinity column was specifically recognized by anti-nucleolin antibody. To confirm that nucleolin was binding to intimin-γ, we next carried out protein overlay experiments. Intimin-γ or intimin-γ carboxyl-terminal third, subjected to nonreducing SDS-PAGE and blotted onto nitrocellulose, were incubated with HEp-2 cell extracts containing nucleolin. Nucleolin that reacted with immobilized intimin-γ was detected with monoclonal anti-nucleolin antibody and a HRP-conjugated anti-mouse IgG-specific secondary antibody. The results of this experiment are presented in Fig. 2*B*. Both the full-length intimin-γ (97-kDa protein in *lane 1*) and the intimin-γ carboxyl-terminal third (35-kDa protein in *lane 2*) bound nucleolin. No anti-nucleolin binding was detected in lanes that contained full-length intimin-γ (*lane 3*) or the intimin-γ carboxyl-terminal third (*lane 4*) incubated with buffer rather than HEp-2 cell extracts. The smaller molecular weight protein species in *lane 1* represent breakdown fragments of full-length intimin-γ. The higher molecular weight species in *lane 2* represent disulfide-linked multimers of the carboxyl-terminal third of intimin-γ. No binding of nucleolin could be detected when intimin-γ was blotted under reducing conditions (data not shown). These findings confirmed that nucleolin bound to intimin-γ and localized the nucleolin-binding region to the carboxyl-terminal third of

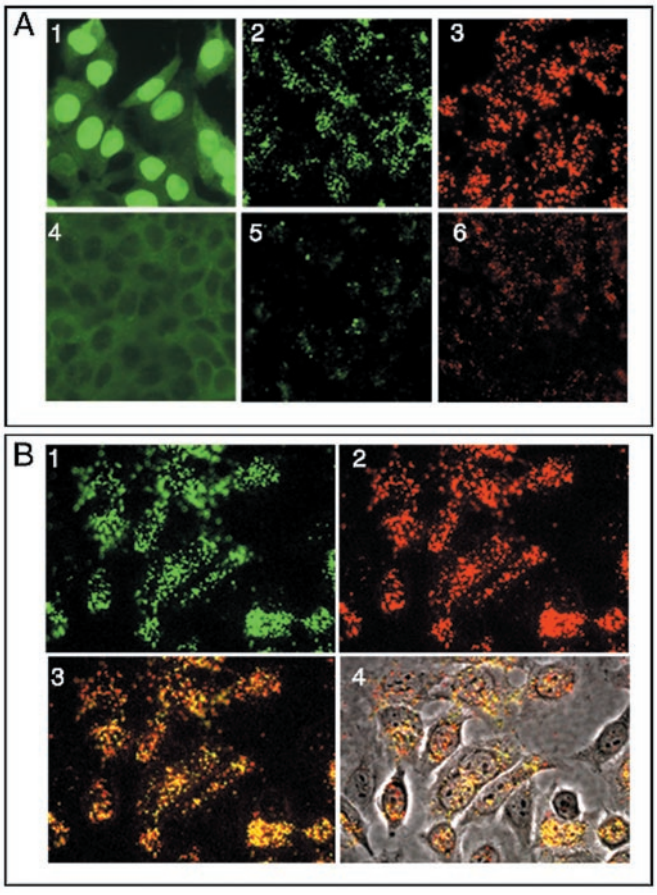

FIG. 3. **Immunofluorescent staining demonstrates similarity between the distribution of nucleolin and bound intimin-γ on the surface of HEp-2 cells.** *A,* HEp-2 cell cultures were stained for nucleolin (*A1, A2, A4*, and *A5*) with mouse anti-nucleolin polyclonal antisera and a FITC-conjugated goat anti-mouse IgG secondary antibody. Nuclear and cytoplasmic nucleolin were stained in fixed/permeabilized cells (*A1, A4*), whereas surface-expressed nucleolin was stained on nonpermeabilized cells (*A2, A5*). In separate wells (*A3, A6*), intimin-γ bound to the cell surface was stained with sheep anti-intimin-γ polyclonal antiserum and Texas Red-conjugated donkey anti-sheep IgG antibody. Subconfluent cells (*A1, A2*, and *A3*) stained brightly for nucleolin in the nucleus (*A1*) and on the cell surface (*A2*) and for bound intimin-γ (*A3*). Confluent cells (*A4, A5*, and *A6*) showed greatly reduced nucleolin staining both in the nucleus (*A4*) and on the surface of the cells (*A5*) and greatly reduced intimin-γ staining (*A6*). *B*, surface-localized nucleolin (*B1*) and bound intimin-γ (*B2*) simultaneously stained on the surface of subconfluent HEp-2 cells. Co-localization of the two proteins is indicated by the predominant *orange-yellow* color when the *red* and *green* staining patterns were overlaid in *panel B3*. These combined patterns are also shown superimposed on the phase-contrast image of the cells in *panel B4*. All images were obtained at an original magnification of 40×.

intimin-γ, the portion of the molecule that contains the putative host cell-binding domain.

Distribution of Nucleolin and Intimin-γ on HEp-2 Cells Is Similar—We reasoned that if nucleolin is indeed a receptor for intimin-γ on HEp-2 cells, then the distribution of these two proteins on the surface of the cells should be similar if not overlapping. To test this hypothesis, we began a series of immunofluorescent staining experiments to investigate the localization of nucleolin and intimin-γ (Fig. 3). For these studies, differentially tagged secondary antibodies were used to indirectly identify nucleolin (stained green with FITC) and intimin-γ (stained red with Texas Red). We first compared the immunostaining patterns of nucleolin within the HEp-2 cells (fixed, permeabilized cells; Fig. 3, *A1* and *A4*) and on the HEp-2 cell surface (nonpermeabilized cells; Fig. 3, *A2* and *A5*) in both subconfluent (Fig. 3, *A1* and *A2*) and confluent cells (Fig. 3, *A4* and *A5*). The intensity of nucleolin staining both in the nucleus and on the cell surface of subconfluent monolayers was much greater than that seen in confluent monolayers and is consistent with the up-regulation of nucleolin expression observed in actively dividing cells (54). In a separate experiment, purified intimin-γ bound to both subconfluent (Fig. 3, *A3*) and confluent HEp-2 cell monolayers (Fig. 3, *A6*) was examined. As predicted, subconfluent cells stained more intensely for bound intimin-γ than did confluent cells. This growth-related difference in nucleolin expression on the cell surface is also in keeping with our previous observation that the intimin-γ receptor concentration decreased as cells reached confluence (Fig. 1). Overall, the patterns of staining for both nucleolin and intimin-γ were similar, and both molecules appeared to be dispersed in a punctate manner over the cell surface (compare *panels A2* and *A3* in Fig. 3). According to a previous report by Frankel and colleagues (12), this punctate staining pattern is characteristic of all intimin subtypes. To show co-localization of nucleolin and intimin-γ on the HEp-2 cell surface, we next simultaneously stained cells for both nucleolin (Fig. 3, *B1*) and intimin-γ (Fig. 3, *B2*). As evident by the yellow-orange color apparent after the anti-nucleolin and anti-intimin-γ images are superimposed (Fig. 3, *B3*), nucleolin and intimin-γ overlap in many regions on the surface of subconfluent HEp-2 cell monolayers. When the staining patterns of both proteins were overlaid on a phase-contrast photomicrograph of the HEp-2 cells (Fig. 3, *B4*), it was clear that the staining did not cover the entire cell surface but was restricted to discrete regions. In fact, some cells showed no apparent staining for either protein, a result that suggests that even in subconfluent monolayers not all HEp-2 cells express nucleolin on the cell surface or can bind intimin-γ.

Nucleolin Is Involved in the Adherence of EHEC O157:H7 to HEp-2 Cells—To address whether intimin-γ on EHEC O157:H7 interacts with nucleolin on the surface of HEp-2 cells during bacterial adherence, a second series of indirect immunofluorescent experiments were done. A comparison of the surface expression of nucleolin in infected HEp-2 cell monolayers (Fig. 4, *A2*) with the distribution of adherent bacterial microcolonies on infected cells (Fig. 4, *A1*) indicated a positive correlation between the regions of nucleolin expression and the areas of bacterial attachment (Fig. 4, *A3* and *A4*). Although FITC-stained nucleolin was evident at the periphery of bacterial microcolonies, the nucleolin stain was not observed beneath intimately adherent bacteria. Moreover, nucleolin was not apparent beneath the bacteria even after permeabilization and staining of infected HEP-2 cells with anti-nucleolin antiserum (data not shown).

The absence of nucleolin staining beneath microcolonies is unlike published reports of actin (56) and Tir (29) accumulation beneath EHEC microcolonies. Although nucleolin appeared to concentrate around the periphery of the microcolony (Fig. 4, *B1* and *B2*), Tir staining was found directly beneath the adherent bacteria (Fig. 4, *B3*) with very little overlap apparent between the two proteins (Fig. 4, *B4*). In similar experiments with infected HEp-2 cells double-stained for nucleolin and intimin-γ, little or no intimin-γ was observed in association with EHEC microcolonies (Fig. 4, *C1* and *C3*), whereas nucleolin was localized around adherent bacterial microcolonies (Fig. 4, *C2* and *C4*). Although some isolated EHEC were brightly stained with the anti-intimin-γ antiserum, most bacteria were not. These results suggest that intimin-γ expression is down-regulated in adherent EHEC, similar to reports of reduced intimin-α expression in EPEC after intimate adherence (57).

EHEC O157:H7 Adherence Is Partially Blocked by Polyclonal Antiserum against Human Nucleolin—Next we asked whether

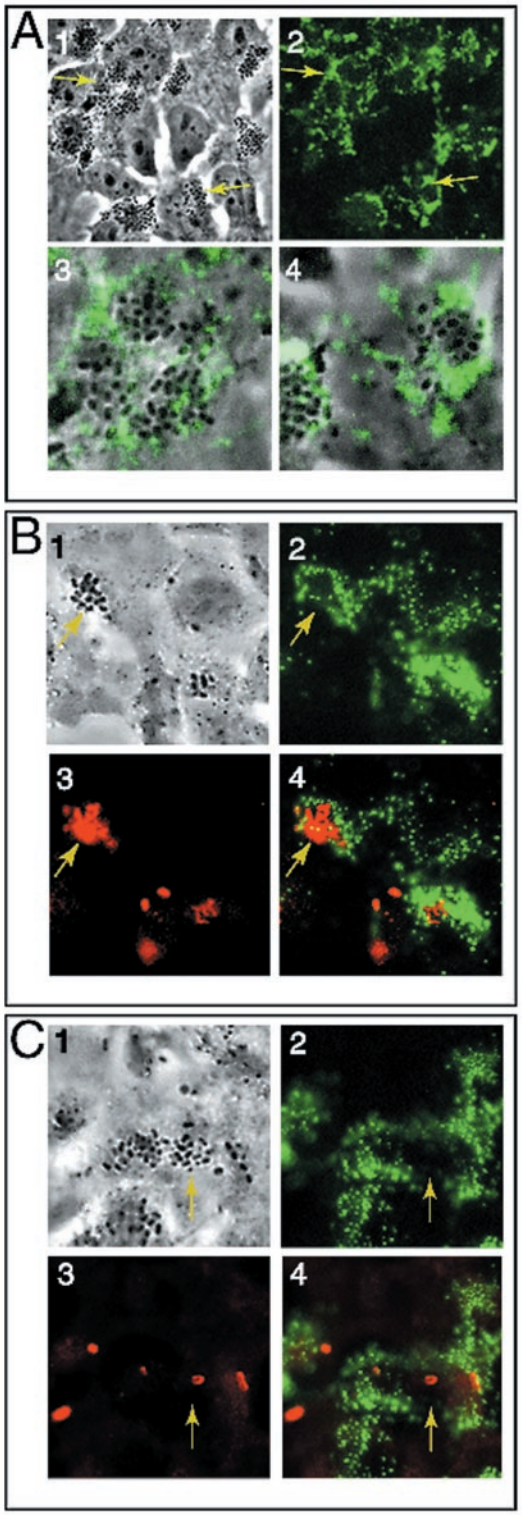

FIG. 4. **EHEC O157:H7 adherence coincides with regions of nucleolin expression on the surface of HEp-2 cells.** Subconfluent HEp-2 cell monolayers were infected with EHEC strain 86-24 for 3 h. Anti-nucleolin sera were added to the infected cells to label surface-localized nucleolin. The bacterial infection was allowed to proceed for an additional 2 h, and the monolayers were then fixed and permeabilized. Anti-nucleolin antibodies bound to nucleolin were detected with a FITC-conjugated goat anti-mouse IgG secondary antibody (panels *A–C*). Tir (*B*) and intimin-γ (*C*) were detected with polyclonal rabbit or sheep antiserum, respectively, and the appropriate Texas Red-conjugated secondary antibody after cell fixation and permeabilization. The *arrows* in each panel denote representative bacterial microcolonies. *A,* phase-contrast image of bacteria adherent to HEp-2 cells (*A1*) and fluorescence microscopy of the same field to show surface nucleolin distribution (*A2*). The regions indicated by *arrows* (*A2*) were superimposed and enlarged (4.5× original magnification) to demonstrate the coincidence of adherent bacteria with nucleolin staining (*A3* and *A4*). All micrographs were taken with a 40× objective *B,* 100× magnification of a phase-contrast micrograph of adherent bacteria (*B1*). Fluorescent microscopy of surface-expressed nucleolin (*B2*), Tir localized beneath adherent bacteria (*B3*), and the two latter images superimposed to indicate regions of overlap (*B4*). *C,* 100× magnification of a phase-contrast micrograph of adherent bacteria (*C1*). Fluorescent microscopy of surface-localized nucleolin (*C2*), intimin-γ (*C3*), and the two staining patterns superimposed (*C4*).

mouse anti-nucleolin antibodies could reduce adherence of EHEC strain 86-24 to HEp-2 cells. First we tested the commercially available anti-nucleolin monoclonal antibody for its adherence-blocking activity. Because of the high level of surface nucleolin expressed in actively dividing cells, confluent HEp-2 cell monolayers were selected for use in these studies to ensure that the concentration of surface-expressed nucleolin was low enough to be saturable with the anti-nucleolin sera. No reduction in EHEC O157:H7 adherence to HEp2 cells was evident in the presence of the monoclonal anti-nucleolin antibody (data not shown). We interpreted this finding to mean that the nucleolin epitope recognized by the monoclonal antibody is distinct from the site on nucleolin to which intimin-γ binds.

Second, we evaluated mouse polyclonal anti-nucleolin sera that we had been raised against SDS-PAGE-purified human nucleolin. To demonstrate that the polyclonal sera was specific for only nucleolin, HEp-2 cell extracts were separated by two-dimensional gel electrophoresis (Fig. 5*A*) and probed with either a monoclonal anti-nucleolin antibody (Fig. 5*B*) or our polyclonal anti-nucleolin sera (Fig. 5*C*). Examination of the autoradiographs of the Western blots revealed that the monoclonal anti-nucleolin antibody and the polyclonal anti-nucleolin sera recognized the same single-protein spot of 110 kDa. Therefore, we concluded that the polyclonal antisera specifically bound nucleolin and no other HEp-2 cell proteins.

We then assessed the adherence-blocking activity of the mouse polyclonal anti-nucleolin sera. As shown in Fig. 6, the adherence-blocking capacity of the anti-nucleolin sera (Fig. 6*B*) against GFP-expressing EHEC strain 86-24 was substantially greater than that of normal mouse sera (Fig. 6*A*). To deplete these sera of anti-nucleolin antibodies, identical dilutions of the anti-nucleolin sera and normal mouse sera were incubated with a preparation of purified nucleolin that had been subjected to preparative SDS-PAGE and blotted onto nitrocellulose. For each sample, the number of adherent bacteria is presented graphically in Fig. 6*C*. Although the anti-nucleolin polyclonal sera decreased the number of adherent bacteria by approximately 7-fold, the same sera that had been depleted of anti-nucleolin antibodies showed no blocking capacity above that seen with normal mouse serum. Additionally, antibodies specific for nucleolin were acid-eluted from the strips of immobilized protein and tested for blocking ability. These monospecific anti-nucleolin antibodies significantly ($p < 0.00001$) decreased the numbers of adherent bacteria when compared with the antibodies that had nonspecifically bound to and been eluted from the nucleolin strips after incubation with normal serum (77 ± 12 bacteria/10 cells for monospecific anti-nucleolin antibodies and 124 ± 16 bacteria/10 cells for the control antibodies from normal mouse serum).

Addition of the polyclonal anti-nucleolin sera 1 h before or concurrent with the addition of bacteria was shown to provide the highest level of blocking activity. When anti-nucleolin sera were added to HEp-2 cells 2 h post-infection, the blocking capacity of the anti-nucleolin antisera was reduced considerably. Typically, in EHEC O157:H7 adherence assays, intimately attached bacteria are not evident until 3–4 h post-infection. The finding that the blocking capacity of polyclonal

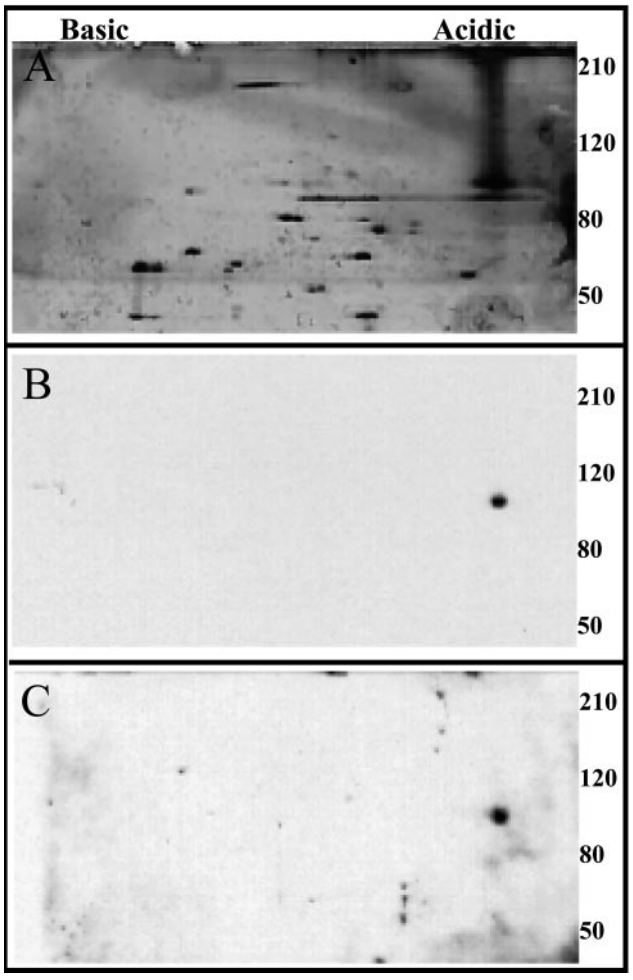

FIG. 5. **Two-dimensional gel electrophoresis reveals specificity of polyclonal mouse anti-nucleolin sera.** Detergent-extracted HEp-2 cellular proteins were separated first by isoelectric point then by molecular weight in a conventional two-dimensional polyacrylamide gel. *A,* silver-stained two-dimensional SDS-polyacrylamide gel of the total protein that was blotted onto nitrocellulose. *B,* Western blot of the HEp-2 cell proteins separated by two-dimensional SDS-PAGE (as in *panel A*) and probed with monoclonal anti-nucleolin antibody. *C,* Western blot of the HEp-2 proteins separated by two-dimensional SDS-PAGE (as in *panel A*) and probed with polyclonal anti-nucleolin sera. Molecular weight markers (in kDa) are indicated on the *right* in each panel.

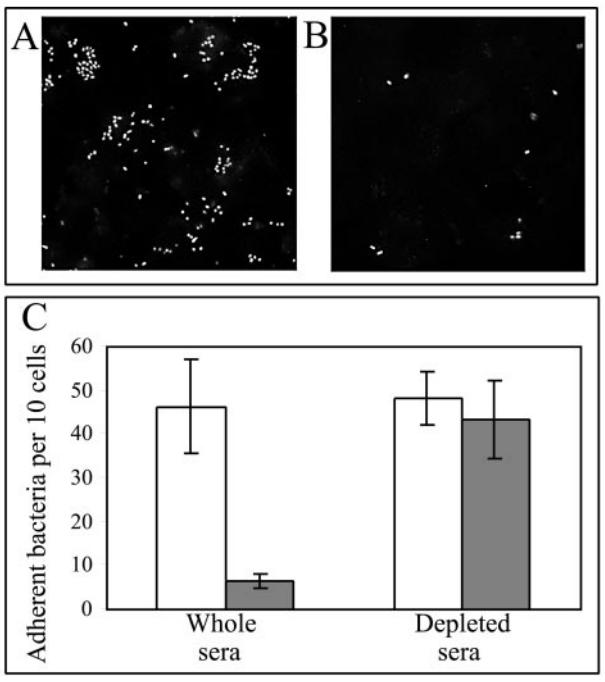

FIG. 6. **Anti-nucleolin antibodies block adherence of EHEC O157:H7 to confluent HEp-2 cells.** Quiescent HEp-2 cell monolayers were treated with either a 1:100 dilution of anti-nucleolin antisera or an equivalent amount of normal mouse sera 1 h prior to infection with GFP-expressing EHEC strain 86-24. After 4 h of infection, nonadherent bacteria were removed and cells were fixed with formalin. Fluorescence micrographs of GFP-expressing bacteria bound to HEp-2 cells are shown for cells treated with normal mouse sera (*A*) or with anti-nucleolin sera (*B*). Each image (obtained at a magnification of 40×) reflects a field of ~50 HEp-2 cells. A 1:100 dilution of the pooled antisera was depleted of anti-nucleolin antibodies by adsorption against purified nucleolin protein immobilized on nitrocellulose. The same dilution of normal mouse sera was also absorbed against purified nucleolin to serve as a control. A total of 48 images like those shown in *panels A* and *B* were obtained for respective samples, and the number of adherent bacteria was counted in each image. The mean number of adherent bacteria per 10 HEp-2 cells is presented in *panel C* for the 1:100 dilution of whole sera (*left columns*) or sera depleted of anti-nucleolin antibodies (*right columns*). The number of adherent bacteria remained essentially unchanged when normal mouse sera (*open columns*) was absorbed against nucleolin, whereas the blocking capacity of the anti-nucleolin sera (*shaded columns*) was abolished when absorbed against purified nucleolin, a finding that presumably reflects loss of anti-nucleolin antibodies. The *error bars* encompass the 98% confidence level for determination of the mean.

anti-nucleolin was reduced if antisera were added after infection but before the appearance of intimately adherent bacteria suggests that the antibodies interfere with the initial association between the bacteria and the host cell surface. If the bacteria had established contact with the HEp-2 cell surface prior to anti-nucleolin addition, then the antisera were not able to block intimate adherence of EHEC. Finally, because the polyclonal anti-nucleolin sera were neither bacteriostatic nor cross-reactive with bacterial cell surface proteins, we believe that the reduction in bacterial adherence to HEp-2 cells in the presence of this reagent is attributable solely to the antisera preventing or reducing the contact between the bacteria and nucleolin on the host cell surface.

DISCUSSION

The question of whether intimin isolated from EPEC or EHEC O157:H7 can directly bind to host cells without Tir, the bacteria-encoded intimin-binding protein, has been the subject of considerable controversy (7). In this investigation, we confirmed the findings of Frankel and colleagues (12, 35), who previously reported Tir-independent interactions of several different intimin types with HEp-2 cells, and we extended these observations by the identification of a candidate receptor for intimin-γ on HEp-2 cells. That nucleolin is in fact this receptor is supported by four lines of evidence from this study. First, a protein with an apparent molecular mass of 110 kDa that bound intimin-γ was isolated from HEp-2 cell extracts and identified by amino acid sequence analysis as nucleolin. Second, immunofluorescent staining of nucleolin and bound intimin-γ strongly suggests co-localization of the two proteins on the HEp-2 cell surface. Third, as demonstrated by immunofluorescence, the sites of EHEC O157:H7 microcolony formation on HEp-2 cells were coincident with areas of nucleolin expression on the cell surface. Fourth, antibodies raised against nucleolin significantly reduced binding of EHEC O157:H7 to HEp-2 cells, with the reduction in adherence most evident when antibodies were added before or at the time of bacterial infection. This last result indicates that the proposed nucleolin/intimin-γ interaction occurs early in the infectious process.

That nucleolin can be found not only in the nucleus but also on the surface of cells has been reported previously (reviewed in Ref. 42). Indeed, Deng *et al*. (47) have documented the

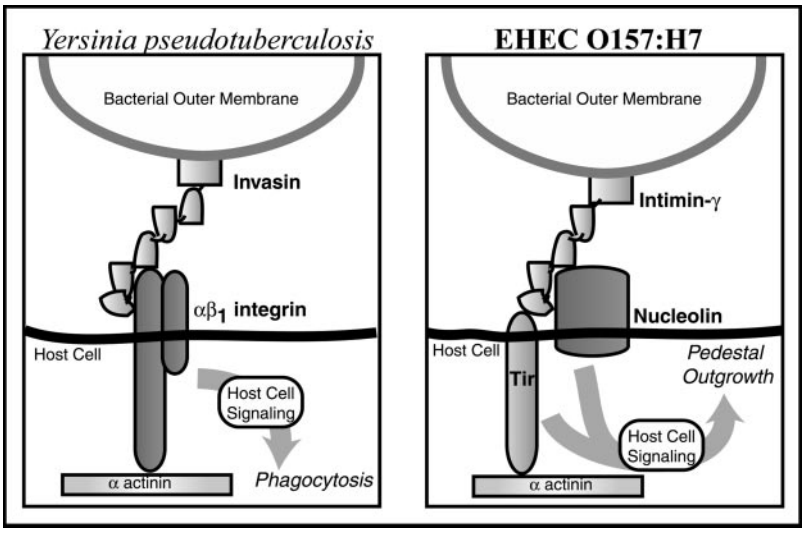

FIG. 7. **Depiction of bacterial adherence mediated by the adhesins invasin and intimin-γ.** The host cell binding domains of invasin and intimin-γ are structurally related (60, 61) and show some similarities in interactions with host cells. Specifically, both invasin and intimin-γ bind to eukaryotic receptors that recognize the extracellular matrix protein laminin, and both proteins evoke an extracellular signaling response from the host cell through receptor-mediated interactions with the cytoskeleton (8, 73). Invasin signals the host cell through β_1 integrin, and this interaction results in internalization of the bacterium. Intimin-γ signals the host cell through Tir, an interaction that results in formation of an actin-rich pedestal that intimately attaches the bacterium to the cell surface. Because of findings that nucleolin may be involved in transmission of signals from the cell surface to the nucleus (42, 48, 54, 64), we propose that the interaction between intimin-γ and nucleolin may also be involved in the host cell response that leads to pedestal formation.

presence of nucleolin on the surface of HEp-2 cells, the cell line used in this study. Furthermore, we observed that there was a higher concentration of nucleolin on the surface of actively dividing cells than on quiescent cells. This finding is consistent with what is known about nucleolin and its turnover in cells, specifically that nucleolin is integral to cell growth and when cell division ceases nucleolin is down-regulated to very low levels in the cell (53, 54). The significant difference in the levels of surface nucleolin expression in active and quiescent cells as noted in this investigation may in part account for the discordant results among published reports on the binding of intimin-γ to uninfected host cells. Perhaps those investigators who observed Tir-independent binding of intimin to cells used subconfluent monolayers in their experiments, whereas researchers who reported only Tir-dependent binding used cells at a higher density for their studies (12, 29, 36).

Although we were able to block the binding of EHEC O157:H7 to HEp-2 cells with polyclonal anti-nucleolin sera, we were unable to demonstrate blocking of EHEC adherence with polyclonal anti-Tir serum (data not shown). The latter observation suggests that the intimin-Tir interaction may not occur until after the bacterium is associated with to the host cell surface and that such an interaction may mask any surface-exposed sites on Tir from the potential blocking activity of the anti-Tir antibodies. The fact that Tir but not nucleolin was present beneath tightly adherent bacteria suggests that the interaction between intimin-γ and nucleolin may become unnecessary once the bacteria are intimately adherent to the host cell surface.

Our analysis showed that nucleolin bound to the carboxyl-terminal portion of intimin-γ, a region of intimin that contains the putative host cell binding domain. We also demonstrated that the interaction between purified intimin-γ and surface-bound receptor gave an apparent dissociation constant of 9×10^{-8} M. This affinity is ~10-fold lower than the association of invasin with its eukaryotic receptor (58). Invasin is homologous to intimin (13) and is used by *Y. pseudotuberculosis* to gain entry into the host cell cytoplasm (11). Invasin binds to β_1 integrin on the cell surface, and this interaction promotes uptake of the bacterium into the cell (14). Tran and Isberg (59) have reported that mutations in invasin that decreased affinity for the receptor also showed decreased numbers of bacteria inside the host cell. EHEC O157:H7 is an extracellular pathogen. We speculate that the weaker affinity of intimin-γ for its eukaryotic receptor may help prevent bacterial internalization by the host cell.

The host cell binding domain of intimin-α is structurally similar to invasin despite little sequence similarity (34, 60, 61). The structure of intimin-γ has not been solved; however, based on sequence similarities between intimin-α and intimin-γ, we assume that intimin-γ also shares a similar conformation. Research with invasin provides clues about specific interactions that may occur between intimin-γ and nucleolin. When invasin is bound to β_1 integrin, binding of the extracellular matrix proteins fibronectin and laminin to these integrins is blocked (58, 62). Invasin binding to $\alpha_3\beta_1$ integrin displaces laminin-5, a result that suggests invasin and laminin-5 have sterically overlapping or identical binding sites (63). Nucleolin, like some integrins, also binds laminin (46, 64). Specifically, nucleolin binds the neurite-promoting site of the A chain of laminin-1 (46). This IKVAV sequence of laminin-1, when synthesized as a peptide, promotes cell attachment, migration, and neurite outgrowth (65). Based on the structural similarities between intimin and invasin, and the finding that invasin and laminin share the same binding site on integrin, we propose that intimin-γ may occupy a position which overlaps the laminin binding site on nucleolin. In pointing out these similarities, we do not mean to imply that intimin-γ and invasin share the same laminin binding site. Rather, we are suggesting that invasin and intimin-γ have evolved to take advantage of two separate laminin receptors on the host cell surface.

A hallmark feature of the A/E lesion produced by intimin-bearing EHEC O157:H7 or EPEC involves outgrowth from the host cell surface of an actin-rich pedestal that cups the bacterium (8). The current model for this pedestal formation involves recruitment of a host cell GTPase by Tir bound to intimin (66). In this model intimin plays a secondary role, acting only to focus Tir beneath the bacteria. Our finding that intimin-γ bound specifically to nucleolin has led us to speculate that intimin-γ may play an additional role in pedestal forma-

tion. We propose that cell-bound intimin-γ may trigger a response in the host cell similar to that which occurs when the cell encounters laminin, *e.g.* the extension of filopodia from the cell surface (65, 67–70). A similar proposal has been made by Phillips *et al.* (71) to explain the observation that latex beads coated with intimin-α induce the formation of microvillus-like processes on the surface of HEp-2 cells. Based on these new findings, we present the following model for EHEC adherence (Fig. 7). Initially intimin-γ on the surface of EHEC would bind to nucleolin in a manner analogous to that of invasin binding to β_1 integrin. This initial adherence, in conjunction with the actions of other bacterial virulence factors (such as the EspA filament (25)), would allow the bacterium to insert Tir into the host cell membrane. Intimin-γ association with both nucleolin and Tir would then trigger a host cell response leading to pedestal formation. This interaction would be similar to the manner in which invasin signals through integrins (26) but with a different outcome. Although our model is speculative, activation of cellular signal transduction pathways through both nucleolin and Tir would explain why intimin-γ requires both a eukaryotic receptor and a bacterially expressed binding partner to facilitate formation of the pedestal. Overall, we feel this research may increase the understanding of similarities between the binding of intimin and invasin to host cell receptors and may suggest how members of this family of proteins have been modified to accommodate different pathogenic strategies.

Acknowledgments—We thank W. Day for providing plasmid p166, L. Gansheroff for advice on the bacterial adherence and protein binding assays and for helpful discussions, S. Darnell for assisting in preparation of anti-nucleolin sera, M. Mills for advice on cell culture, and K. Meysick for helpful comments on this manuscript. We acknowledge L. Dangott and the Protein Chemistry Laboratory at Texas A&M University for advice on protein sequencing methods and for providing excellent service in the sequencing of nucleolin.

REFERENCES

1. Mead, P. S., Slutsker, L., Dietz, V., McCaig, L. F., Bresee, J. S., Shapiro, C., Griffin, P. M., and Tauxe, R. V. (1999) *Emerg. Infect. Dis.* **5,** 607–625
2. Jerse, A. E., Yu, J., Tall, B. D., and Kaper, J. B. (1990) *Proc. Natl. Acad. Sci. U. S. A.* **87,** 7839–7843
3. Levine, M. M. (1987) *J. Infect. Dis.* **155,** 377–389
4. Kenny, B., De Vinney, R., Stein, M., Reinscheid, D. J., Frey, E. A., and Finlay, B. B. (1997) *Cell* **91,** 511–520
5. McDaniel, T. K., Jarvis, K. G., Donnenberg, M. S., and Kaper, J. B. (1995) *Proc. Natl. Acad. Sci. U. S. A.* **92,** 1664–1668
6. Jarvis, K. G., Giron, J. A., Jerse, A. E., McDaniel, T. K., Donnenberg, M. S., and Kaper, J. B. (1995) *Proc. Natl. Acad. Sci. U. S. A.* **92,** 7996–8000
7. Frankel, G., Phillips, A. D., Rosenshine, I., Dougan, G., Kaper, J. B., and Knutton, S. (1998) *Mol. Microbiol.* **30,** 911–921
8. Goosney, D. L., de Grado, M., and Finlay, B. B. (1999) *Trends Cell Biol.* **9,** 11–14
9. Jerse, A. E., and Kaper, J. B. (1991) *Infect. Immun.* **59,** 4302–4309
10. Kaper, J. B., Gansheroff, L. J., Wachtel, M. R., and O'Brien, A. D. (1998) in *Escherichia coli O157:H7 and Other Shiga Toxin-producing E. coli Strains* (Kaper, J. B., and O'Brien, A. D., eds) pp. 148–156, ASM Press, Washington, D. C.
11. Isberg, R. R., Voorhis, D. L., and Falkow, S. (1987) *Cell* **50,** 769–778
12. Frankel, G., Candy, D. C., Everest, P., and Dougan, G. (1994) *Infect. Immun.* **62,** 1835–1842
13. McGraw, E. A., Li, J., Selander, R. K., and Whittam, T. S. (1999) *Mol. Biol. Evol.* **16,** 12–22
14. Isberg, R. R., and Leong, J. M. (1990) *Cell* **60,** 861–871
15. Batchelor, M., Prasannan, S., Daniell, S., Reece, S., Connerton, I., Bloomberg, G., Dougan, G., Frankel, G., and Matthews, S. (2000) *EMBO J.* **19,** 2452–2464
16. Adu-Bobie, J., Frankel, G., Bain, C., Goncalves, A. G., Trabulsi, L. R., Douce, G., Knutton, S., and Dougan, G. (1998) *J. Clin. Microbiol.* **36,** 662–668
17. Oswald, E., Schmidt, H., Morabito, S., Karch, H., Marches, O., and Caprioli, A. (2000) *Infect. Immun.* **68,** 64–71
18. Donnenberg, M. S., Tzipori, S., McKee, M. L., O'Brien, A. D., Alroy, J., and Kaper, J. B. (1993) *J. Clin. Invest.* **92,** 1418–1424
19. Hicks, S., Frankel, G., Kaper, J. B., Dougan, G., and Phillips, A. D. (1998) *Infect. Immun.* **66,** 1570–1578
20. Phillips, A. D., Navabpour, S., Hicks, S., Dougan, G., Wallis, T., and Frankel, G. (2000) *Gut* **47,** 377–381
21. Tzipori, S., Gunzer, F., Donnenberg, M. S., de Montigny, L., Kaper, J. B., and Donohue-Rolfe, A. (1995) *Infect. Immun.* **63,** 3621–3627
22. McKee, M. L., Melton-Celsa, A. R., Moxley, R. A., Francis, D. H., and O'Brien, A. D. (1995) *Infect. Immun.* **63,** 3739–3744
23. Dean-Nystrom, E. A., Bosworth, B. T., Moon, H. W., and O'Brien, A. D. (1998) *Infect. Immun.* **66,** 4560–4563
24. Gansheroff, L. J., Wachtel, M. R., and O'Brien, A. D. (1999) *Infect. Immun.* **67,** 6409–6417
25. Knutton, S., Rosenshine, I., Pallen, M. J., Nisan, I., Neves, B. C., Bain, C., Wolff, C., Dougan, G., and Frankel, G. (1998) *EMBO. J.* **17,** 2166–2176
26. Isberg, R. R., Hamburger, Z., and Dersch, P. (2000) *Microbes Infect.* **2,** 793–801
27. Frankel, G., Lider, O., Hershkoviz, R., Mould, A. P., Kachalsky, S. G., Candy, D. C. A., Cahalon, L., Humphries, M. J., and Dougan, G. (1996) *J. Biol. Chem.* **271,** 20359–20364
28. Liu, H., Magoun, L., and Leong, J. M. (1999) *Infect. Immun.* **67,** 2045–2049
29. De Vinney, R., Stein, M., Reinscheid, D., Abe, A., Ruschkowski, S., and Finlay, B. B. (1999) *Infect. Immun.* **67,** 2389–2398
30. Phillips, A. D., and Frankel, G. (2000) *J. Infect. Dis.* **181,** 1496–1500
31. Perna, N. T., Mayhew, G. F., Posfai, G., Elliott, S., Donnenberg, M. S., Kaper, J. B., and Blattner, F. R. (1998) *Infect. Immun.* **66,** 3810–3817
32. Frankel, G., Candy, D. C., Fabiani, E., Adu-Bobie, J., Gil, S., Novakova, M., Phillips, A. D., and Dougan, G. (1995) *Infect. Immun.* **63,** 4323–4328
33. Frankel, G., Philips, A. D., Novakova, M., Batchelor, M., Hicks, S., and Dougan, G. (1998) *Mol. Microbiol.* **29,** 559–570
34. Luo, Y., Frey, E. A., Pfuetzner, R. A., Creagh, A. L., Knoechel, D. G., Haynes, C. A., Finlay, B. B., and Strynadka, N. C. (2000) *Nature* **405,** 1073–1077
35. Hartland, E. L., Batchelor, M., Delahay, R. M., Hale, C., Matthews, S., Dougan, G., Knutton, S., Connerton, I., and Frankel, G. (1999) *Mol. Microbiol.* **32,** 151–158
36. Liu, H., Magoun, L., Luperchio, S., Schauer, D. B., and Leong, J. M. (1999) *Mol. Microbiol.* **34,** 67–81
37. McKee, M. L., and O'Brien, A. D. (1996) *Infect. Immun.* **64,** 2225–2233
38. Guzman, L. M., Belin, D., Carson, M. J., and Beckwith, J. (1995) *J. Bacteriol* **177,** 4121–4130
39. Cormack, B. P., Valdivia, R. H., and Falkow, S. L. (1996) *Gene* **173,** 33–38
40. Wilson, B. A., Aminova, L. R., Ponferrada, V. G., and Ho, M. L. (2000) *Infect. Immun.* **68,** 4531–4538
41. Altschul, S. F., Gish, W., Miller, W., Myers, E. W., and Lipman, D. J. (1990) *J. Mol. Biol.* **215,** 403–410
42. Srivastava, M., and Pollard, H. B. (1999) *FASEB J.* **13,** 1911–1922
43. Ginisty, H., Sicard, H., Roger, B., and Bouvet, P. (1999) *J. Cell Sci.* **112,** 761–772
44. Orrick, L. R., Olson, M. O., and Busch, H. L. (1973) *Proc. Natl. Acad. Sci. U. S. A.* **70,** 1316–1320
45. Bugler, B., Caizergues-Ferrer, M., Bouche, G., Bourbon, H., and Amalric, F. L. (1982) *Eur. J. Biochem.* **128,** 475–480
46. Kibbey, M. C., Johnson, B., Petryshyn, R., Jucker, M., and Kleinman, H. K. (1995) *J. Neurosci. Res.* **42,** 314–322
47. Deng, J. S., Ballou, B., and Hofmeister, J. K. (1996) *Mol. Biol. Rep.* **23,** 191–195
48. Zhou, G., Seibenhener, M. L., and Wooten, M. W. (1997) *J. Biol. Chem.* **272,** 31130–31137
49. Sorokina, E. A., and Kleinman, J. G. (1999) *J. Biol. Chem.* **274,** 27491–27496
50. de Verdugo, U. R., Selinka, H. C., Huber, M., Kramer, B., Kellermann, J., Hofschneider, P. H., and Kandolf, R. (1995) *J. Virol.* **69,** 6751–6757
51. Callebaut, C., Blanco, J., Benkirane, N., Krust, B., Jacotot, E., Guichard, G., Seddiki, N., Svab, J., Dam, E., Muller, S., Briand, J. P., and Hovanessian, A. G. (1998) *J. Biol. Chem.* **273,** 21988–21997
52. Lee, C. H., Chang, S. C., Chen, C. J., and Chang, M. F. (1998) *J. Biol. Chem.* **273,** 7650–7656
53. Lapeyre, B., Bourbon, H., and Amalric, F. L. (1987) *Proc. Natl. Acad. Sci. U. S. A.* **84,** 1472–1476
54. Hovanessian, A. G., Puvion-Dutilleul, F., Nisole, S., Svab, J., Perret, E., Deng, J. S., and Krust, B. (2000) *Exp. Cell Res.* **261,** 312–328
55. Erard, M. S., Belenguer, P., Caizergues-Ferrer, M., Pantaloni, A., and Amalric, F. (1988) *Eur. J. Biochem.* **175,** 525–530
56. Knutton, S., Baldwin, T., Williams, P. H., and McNeish, A. S. (1989) *Infect. Immun.* **57,** 1290–1298
57. Knutton, S., Adu-Bobie, J., Bain, C., Phillips, A. D., Dougan, G., and Frankel, G. (1997) *Infect. Immun.* **65,** 1644–1652
58. Van Nhieu, G. T., and Isberg, R. R. (1991) *J. Biol. Chem.* **266,** 24367–24375
59. Tran, V. N., and Isberg, R. R. (1993) *EMBO J.* **12,** 1887–1895
60. Kelly, G., Prasannan, S., Daniell, S., Fleming, K., Frankel, G., Dougan, G., Connerton, I., and Matthews, S. (1999) *Nat Struct. Biol.* **6,** 313–318
61. Hamburger, Z. A., Brown, M. S., Isberg, R. R., and Bjorkman, P. J. (1999) *Science* **286,** 291–295
62. Krukonis, E. S., Dersch, P., Eble, J. A., and Isberg, R. R. (1998) *J. Biol. Chem.* **273,** 31837–31843
63. Eble, J. A., Wucherpfennig, K. W., Gauthier, L., Dersch, P., Krukonis, E., Isberg, R. R., and Hemler, M. E. (1998) *Biochemistry* **37,** 10945–10955
64. Yu, D., Schwartz, M. Z., and Petryshyn, R. L. (1998) *Biochem. Biophys. Res. Commun.* **247,** 186–192
65. Tashiro, K., Sephel, G. C., Weeks, B., Sasaki, M., Martin, G. R., Kleinman, H. K., and Yamada, Y. (1989) *J. Biol. Chem.* **264,** 16174–16182
66. Kalman, D., Weiner, O. D., Goosney, D. L., Sedat, J. W., Finlay, B. B., Abo, A., and Bishop, J. M. (1999) *Nat. Cell Biol.* **1,** 389–391
67. Nobes, C. D., and Hall, A. L. (1995) *Cell* **81,** 53–62
68. Dogic, D., Rousselle, P., and Aumailley, M. L. (1998) *J. Cell Sci.* **111,** 793–802
69. Hall, A. L. (1998) *Science* **279,** 509–514
70. Brown, M. D., Cornejo, B. J., Kuhn, T. B., and Bamburg, J. R. (2000) *J. Neurobiol.* **43,** 352–364
71. Phillips, A. D., Giron, J., Hicks, S., Dougan, G., and Frankel, G. (2000) *Microbiology* **146,** 1333–1344